

# Assessing the impact of dopants on electrokinetic rock properties as potential indicators for dopant induced wettability changes

Matthias Halisch<sup>1,\*</sup>, Fabrice Pairoys<sup>2</sup>, Cyril Caubit<sup>2</sup>, and Thomas Grelle<sup>1</sup>

<sup>1</sup> LIAG, Dept. 5 - Petrophysics & Borehole Geophysics, Stilleweg 2, D-30655 Hannover, Germany

<sup>2</sup> TotalEnergies, CSTJF, Avenue Larribau, 64018 Pau Cedex, France

**Abstract.** The usage of sodium iodide or potassium iodide as contrast enhancing dopant is common practice during laboratory coreflooding experiments in order to support modern 3D imaging techniques and later digital image analysis. It helps to overcome the low phase contrast between water and oil for in-situ saturation monitoring. Pairoys et al. (2023) revealed that dopants seem to play a significant role in wettability alteration, as far as our understanding of crude oil, brine, and rock interaction allows to conclude. As shown, this alteration could introduce a significant bias in SCAL experiments. The results showed a significant dopant impact on oil recovery in clastic rocks, especially during the spontaneous displacement process. To understand the underlying mechanisms, it is important and necessary to characterize the brine-rock-interaction as best as possible, before - in a second step - the understanding of wettability alteration at the oil-water-rock-interface. In this study, three different types of sandstone (Bentheimer, Obernkirchen and Berea) are chosen for a systematic assessment of their related electrokinetic properties by using different dopants and concentrations. As preparation step, all rock samples were fragmented by the so-called lightning-shock fragmentation (selFrag) technique to preserve the in-situ grain topology and surface properties, respectively. The resulting unconsolidated, sieved, and prepared material was used for electroacoustic sound amplitude measurements, following a strict and innovative experimental protocol. This protocol was continuously repeated for different dopants with increasing concentrations (1g/l, to 6g/l, to 12g/l, for NaI, KI, CsCl, and BaCl, respectively). Following this protocol, changes in the electrokinetic properties support the findings of the first mentioned study, underlining the assumption that dopants could bias SCAL experiments.

## 1 Introduction

Because SCAL waterflooding with X-ray saturation monitoring requires doping one phase, [1] investigated the effect of brine containing sodium iodide (NaI) on wettability and the oil recovery factor. The tests consisted of adding varying NaI concentrations in the connate brine (1g/l, 6g/l, 12g/l) and in the injected brine. They showed that:

- If the connate brine is free of NaI, and even if the injected brine contains some, the spontaneous and forced imbibition cycles were similar to the reference test (the reference sample had no NaI, neither in connate nor in injected brine).
- If connate brine does contain NaI, the samples behaved more water-wet than those with no NaI in connate brine, leading to an increase in their water-wetness according to the increased NaI concentration.

All these findings are clearly illustrated in Figure 1. The figure shows that samples without NaI in the connate

brine (Be1, Be2, and Be3) have the same water wettability indices ( $I_w$ ). In contrast, samples with NaI in the connate brine (Be4, Be5, and Be6) have higher  $I_w$  values, which increase with the concentration of NaI.

If the impact of dopants on SCAL waterflooding tests is evident, the question of the mechanisms involved in wettability alteration remains unanswered. Physico-chemical factors, like ionic interaction, deliver explanations for these observations. This paper aims to investigate the brine-rock interaction as a starting-point for a deeper understanding of wettability mechanisms. Assuming that the electrical double layer (EDL) is one mechanism affecting wettability [2, 3, 4, 5], we have developed a unique workflow to evaluate the influence of potential dopants on electrokinetic properties systematically. First, we would like to assess the role of NaI at the brine-surface interface by systematically measuring zeta-potentials for different sandstones. Second, we investigate and assess the impact of

\* Corresponding author: [matthias.halisch@leibniz-liag.de](mailto:matthias.halisch@leibniz-liag.de)

alternative dopants (i.e., solutions with high atomic numbers for phase contrast enhancement, as KI, CsCl, and BaCl) on sample electrokinetics. Third, we compare all results and assess our findings with special regards to the observations made by [1].

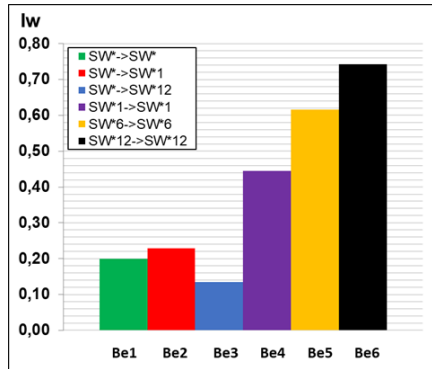


**Fig. 1.**  $I_w$  results as presented by [1]. This plot is probably the most relevant indication of the effect of NaI doping agent on wettability: samples with no NaI in the sitting brine, and despite the doped imbibing brine, have same  $I_w$  between 0.13 and 0.23 (Be1-3). For the samples with NaI in the sitting brines,  $I_w$  are much higher, from 0.44 and 0.74 (Be4-6), with increasing  $I_w$  and with increasing NaI concentration. Important to note that with 1g/l only of NaI in connate water (Be4),  $I_w$  value is double compared to the  $I_w$  values of the tests with no NaI in connate water (Be1, Be2, Be3).

Electrochemical processes and interactions result in a solid accumulation of ions on the surface of the mineral grain. This "solid" layer is called the Stern layer (or Helmholtz layer). The transition to the (free) pore fluid is formed by a region of diffusely distributed ions. The ion concentration within this diffuse layer decreases exponentially with distance from the Stern layer. Together, this results in the so-called electric double layer (EDL, Fig. 2).

The relevant parameter characterizing the diffuse part of the EDL is the so-called zeta potential [2]. The zeta potential is defined as the electric potential at the shear layer of a surface or a particle, moving relatively against an ion bearing liquid. Consequently, the zeta potential is an interfacial property (here at the solid-liquid interface) and depends on the surface potential (or surface charge) and thus on the mineral, its surface, and the properties of the electrolyte [6]. Overall, in a clastic rock-brine system like these sandstones, we can generally assume the  $\text{SiO}_2$  surface to be negatively charged due to the dissociation of silanol groups ( $\text{Si-OH}$ ) and the prevalence of negatively charged silicate ions on the surface, especially under conditions of moderate to high pH [7, 8]. The negative surface charge plays a significant role in influencing the electrokinetic properties, and interactions with dissolved

ions in the aqueous phase. The zeta potential serves as the primary indicator of the electrostatic repulsion (or attraction) of ions in the dispersion medium. A higher zeta potential means greater repulsion, while a lower zeta potential means less repulsion. As a result, higher zeta potential reduces the likelihood of small charged (mineral) particles clumping together and decreases the tendency for liquid phases to exhibit wetting behaviour at the interface [6, 9].

## 2 Samples

### 2.1 Rock Samples

This study utilized three different sandstones: Bentheimer (BE), Berea (BR), and Obernkirchen (OK). The BE sandstone, featured in the initial study by [1], facilitates a direct comparison and connection of results between the two studies. BR and OK sandstones were chosen to introduce slight variations in mineralogy and grain size to the experiment. Additionally, BE and BR samples are frequently employed as proxies or reference rock types for systematic laboratory investigations. The OK sandstone fills the gap between BE and BR in that respect. The Bentheimer sandstone, originating from the Upper Cretaceous period, is known for its widespread occurrence in northern Germany and the Netherlands. Berea sandstone, on the other hand, is a prominent formation found in Ohio, USA, dating back to the Late Devonian to Early Mississippian periods. The Obernkirchen sandstone, sourced from Germany, belongs to the Lower Cretaceous period.

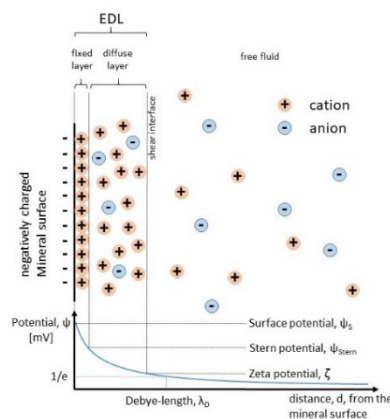


**Fig. 2.** Schematic representation of the charge carrier distribution at the interface between mineral grain (left) and electrolyte (right) without an externally applied electric field. At the negatively charged mineral surface (e.g., quartz) a fixed and a diffuse layer form, which together create the electrical double layer.

These sandstones possess several key features that make them highly suitable for laboratory studies. They exhibit uniform grain size distribution, with porosity values averaging 22% for BE, 19% for BR, and 15% for OK, and good to excellent permeability characteristics, making them ideal candidates for systematic laboratory experiments, e.g., coreflooding or fundamental process characterization. Additionally, their well-defined mineralogical composition allows for precise control and manipulation of experimental parameters, both essential for systematic work on the EDL characterization. The detailed mineralogical composition of our samples is presented in Table 1.

**Table 1.** Mineral composition of the investigated samples.

Mineral	BE	BR	OK
Quartz	95 wt.%	75 wt.%	88 wt.%
K-feldspar	3 wt.%	6 wt.%	2 wt.%
Plagioclase	<< 1 wt.%	5 wt.%	1 wt.%
Muscovite	/	5 wt.%	2 wt.%
Chlorite	/	3 wt.%	/
Kaolinite	2 wt.%	5 wt.%	7 wt.%
Calcite	/	/	/
Dolomite	/	/	/

## 2.2 Dopants & Liquid Solutions

All synthetic solutions were prepared under laboratory conditions to ensure high reproducibility and comparability among the suspensions. Demineralized water served as the base for all solutions. Three dopant concentrations were used: 1g/l, 6g/l, and 12g/l. Sodium iodide (NaI), potassium iodide (KI), cesium chloride (CsCl), and hydrated barium chloride (BaCl) were chosen as potential dopant-alternatives for X-ray monitoring during SCAL experiments, with a chemical purity greater than 99.99%. Iodide solutions were labeled as group A, while chloride solutions were labeled as group B. A 1g/l sodium chloride (NaCl) solution was used for reference measurements at constant concentration only, as it's not a good contrast enhancing dopant (see chapter 3.3) due to its low atomic number, i.e., low X-ray absorption.

Utilizing both, iodides and chlorides offers distinct advantages when investigating zeta potentials. These compounds provide versatility and reliability in experimental settings. Their solubility in water ensures homogeneous dispersion within the solution, which is crucial for consistent and reproducible results. Moreover, these ions possess different properties that influence the electrochemical environment, allowing for exploration of a wide range of conditions. For instance, iodide ions, with their larger size and polarizability, can affect the double

layer structure more significantly compared to smaller ions like chloride [10, 11].

This variation in ion characteristics enables fine-tuning of the solution's ionic strength and composition, thereby systematically influencing the build-up of zeta potential and the corresponding EDL characterization. Additionally, their potential as dopants for enhancing phase contrast during X-ray imaging, with respect to the outcome of this study, is evaluated for general applicability. Table 2 provides a summary of the various liquid solutions employed in this study.

**Table 2.** Dopants and solutions used in this study. Please note: NaCl has been used for reference measurements only; hence, there is only one NaCl-based liquid.

dopant	group	concentration sub-groups		
		1g/l	6g/l	12g/l
NaI	A	A1.1	A1.2	A1.3
KI		A2.1	A2.2	A2.3
NaCl	B	B1.1	/	/
CsCl		B2.1	B2.2	B2.3
BaCl		B3.1	B3.2	B3.3

## 2.3 Suspensions

The experimental setup for this study required suspensions, which were prepared by combining 150 ml of various dopant solutions listed in Table 2 with 3 g of specially prepared rock material (see chapter 3.1) sourced from each of the three sandstones. This ensured that each final suspension contained 2-wt% of rock material, adequate for measuring zeta potentials as elaborated in section 3.2. The rock material has been sieved into two different grain fractions: 60 – 200  $\mu\text{m}$  and < 60  $\mu\text{m}$ . The larger size fraction has been used for this study, assuming that all relevant matrix forming minerals and surfaces have been considered (please note: due to the disaggregation technique, smaller grain sizes are lost during processing anyhow. Hence, this size fraction would be less representative for the rock). Throughout the study, 45 different suspensions were created (five different dopants, three different concentrations for each dopant, multiplied by three different sandstones). Furthermore, the specially prepared and limited amount of rock material was utilized efficiently for this specific type of systematic laboratory experiment.

## 3 Key Methods & Lab Procedures

### 3.1 selfFrag Technique

A key method employed in this study is the electrodynamic disaggregation technique, also known as the "selfFrag" technique, which has been described in detail in previous works [12, 13, 14]. This method enables the fragmentation of rocks, mineral agglomerates, mono-mineral crystals, and glasses along grain boundaries or internal material discontinuities, such as fluid inclusions or dissolution structures. During the electrodynamic disaggregation process, an electrical discharge is directed towards a non- or low-conductive material, such as a rock, while it is immersed in a dielectric fluid, such as water or oil. Normally, the electrical resistance of a solid phase is greater than that of a liquid phase.

However, as soon as a high electrical voltage is applied in short pulses, the physical behavior of the material changes drastically. Under these conditions, the rock behaves as a conductor while the surrounding liquid acts as an insulator. The sample serves as a discharge channel between the cathode and anode of the fragmentation apparatus. As a result, large amounts of energy are accumulated along the sample axis, leading to the generation of a pressure wave that propagates along grain boundaries or surfaces. This wave induces tensile stresses that effectively disaggregate the rock sample without destroying the grains and according surfaces, as demonstrated by [12]. In total, about 200 g of material has been fragmented for each of the sandstones, which equals only about 3 – 4 standard core plugs of material.

### 3.2 Electrokinetic Sound Amplitude Technique

The second key method is the so-called "electrokinetic sonic amplitude effect" (ESA) measurement as introduced in the 2022 symposium of the SCA [12], and described in detail by [15, 16]. Here, this method is briefly described in the following. Figure 3 schematically shows the setup of the instrument. While the suspension is in continuous circulation in the system, an alternating voltage is applied between two plate electrodes (Fig. 3, D), which are in direct contact with the suspension. As the suspension passes through the alternating electric field, the dispersed particles are deflected toward the plates. This produces a measurable ultrasonic wave as all particles move in phase with each other. The ESA wave is decoupled by a silicate glass window (Fig. 3, B) and its amplitude is converted into a signal by a piezoelectric transducer.

The signal depends on the particle velocity and thus consequently on the particle charge, particle size and shape. Larger particles are inert compared to small particles, causing a time delay between the change in direction of the electric field and the direction of particle motion (i.e., a change in sign of the particle velocity). By

measuring the magnitude and phase of the ESA signal, both the zeta potential and the particle size can be determined [17]. As the particle size distribution for this study is well known, only zeta potentials have been calculated. The main advantage of the ESA method is that significantly larger particle (grain) sizes can be included for systematic investigations of natural rocks. Whereas classical methods are strictly limited regarding this parameter, ESA is able to include grains as large as up to 200-300  $\mu\text{m}$  in diameter (i.e., at least 100 times larger grains than electrophoresis).

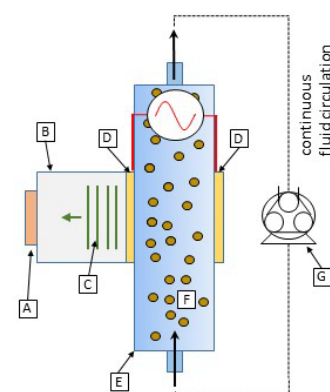


**Fig. 3.** Schematic illustration of the method as introduced by [12]. (A) Piezoelectric transducer, (B) high-purity silicate glass, (C) ESA shaft, (D) plate electrodes, (E) measuring cell, (F) suspension, (G) peristaltic metering pump.

From these experiments, zeta potential values are derived using the concept of electrodynamic mobility, a fundamental parameter in electrokinetics. Electrodynamic mobility ( $\mu$ ) represents the velocity of charged particles moving through the fluid under an applied electric field. It is directly measured in our experimental setup and serves as a dynamic indicator of particle behavior in the fluid medium. Experimental parameters such as the electrical field strength ( $E$ ), the permittivity of the liquid medium ( $\epsilon$ ), and the viscosity of the liquid medium ( $\eta$ ) are known or closely assumed constants. While the electrical field strength can be controlled and measured, the permittivity and viscosity of the medium (typically water) are well-characterized properties. Considering the drag on the moving particles due to the viscosity of the dispersant, in the case of low Reynolds number and moderate electric field strength  $E$ , the drift velocity of a dispersed particle ( $v$ ) is simply proportional to the applied field, which leaves the electrophoretic mobility ( $\mu_e$ ) defined as:

$$\mu_e = v/E \quad (1)$$

Marian Smoluchowski developed the most well-known and widely used theory of electrophoresis in 1903 [18, 19]. This theory describes the relationship between

electrodynamic mobility ( $\mu$ ), zeta potential ( $\zeta$ ), and other parameters as follows:

$$\zeta = \mu \eta / \epsilon_r \epsilon_0 \quad (2)$$

Where  $\epsilon_r$  is the dielectric constant of the dispersion medium,  $\epsilon_0$  is the permittivity of free space (given in  $\text{C}^2\text{N}^{-1}\text{m}^{-2}$ ),  $\eta$  is the dynamic viscosity of the dispersion medium (Pa s), and  $\zeta$  is the zeta potential (typically measured in mV). The Smoluchowski theory is very powerful because it works for dispersed particles of any shape at any concentration.

### 3.3 Laboratory Procedure

The developed experimental procedure involves three main steps: sample preparation, fluid and suspension preparation (as described in sections 2.2, 2.3, and 3.1), and ESA measurements (as elaborated in section 3.2). While the first two steps are straightforward, the demands for the ESA instrumentation and measurement cycles are significantly higher.

The equipment needs to be calibrated twice per day or if the temperature in the laboratory environment exceeds a change of 3 °C. A special calibration liquid with well-known properties for polar media is used to compensate for drift and stability of the measurement. For each suspension, a so-called background measurement has been performed to account for any potential interference or contamination that could affect the accuracy of the experimental results. The apparent (or uncorrected) zeta potential is the direct measurement of the electrokinetic potential of particles in a suspension without any corrections. It includes the contributions from both the particles and the fluid medium. It can vary significantly with changes in the fluid's ionic strength and composition. It is useful for quick assessments where high precision is not critical or when the fluid composition is constant and well understood.

The background-corrected zeta potential is obtained by subtracting the background signal (the electroacoustic properties of the fluid without particles) from the apparent zeta potential. This correction isolates the true electrokinetic potential of the particles, removing any interference from the fluid medium. It provides a more accurate measure of the particles' electrokinetic behavior by eliminating the fluid's influence, and is essential for comparing the zeta potentials of particles in different fluid compositions or concentrations, as it ensures that only the particle properties are measured.

As for our case study, when conducting measurements with different concentrations of the same salt in the fluid, the background correction is crucial for meaningful comparison. Higher salt concentrations can compress the electrical double layer around particles, altering the apparent zeta potential. Without background correction, it is challenging to discern whether changes in zeta potential are due to particle properties or fluid interactions. As an example: Two samples with different salt concentrations can show different zeta potentials due to the varying ionic strength of the fluid. After correcting for the fluid's influence, any differences in zeta potential can be attributed to the particles themselves, providing a clearer understanding of how the salt concentration affects particle behavior.

Comparing apparent and background-corrected zeta potentials is meaningful and necessary for precise electrokinetic studies. The apparent zeta potential offers a quick overview, but the background-corrected value provides a detailed, accurate assessment crucial for understanding particle behavior in varying fluid conditions. For our study, we will present both, uncompensated (i.e., apparent) and compensated (i.e., background corrected) zeta potentials. More details on the background correction methodology for assessing ESA measurements can be found in [15, 16].

The measurements followed the same protocol for each of the investigated sample materials. First, a reference measurement with 1g/l NaCl (suspension B1.1) was conducted. These reference measurements are subsequently re-done in between the dopant cycles, using the same NaCl concentration of 1g/l. If this "ground truth" reference changes throughout the experiment, these irreversible changes are directly related to the according dopant used before. The sandstone material was sieved, cleaned with demineralized water, and oven-dried at 75°C for 1 hour before being reused for the first dopant suspension (e.g., NaI at the lowest concentration). After this run, the material was sieved, cleaned, and dried again as described, followed by another reference measurement using B1.1. This cyclic procedure was then repeated with stepwise increasing concentrations for each different dopant and rock sample. During one complete dopant cycle (i.e., from lowest to highest dopant concentration), the loss of sample material was investigated between each cleaning and drying. New sample material was used only if the type of dopant changed (i.e., from NaI to KI). By adhering to this strict protocol and conducting repeated reference runs before advancing to the next concentration, any dopant-induced changes in the material could be readily identified. Additionally, this approach helped

prevent cross-contamination of the rock material. Both of these points are crucial for achieving reliable and reproducible data on the impact of dopants for each of the sandstone samples.

Finally, all measured data have been processed, including the calculation of Smoluchowski zeta potentials (see section 3.2), and background corrections have been applied. Figure 4 provides a visual representation of this comprehensive workflow.

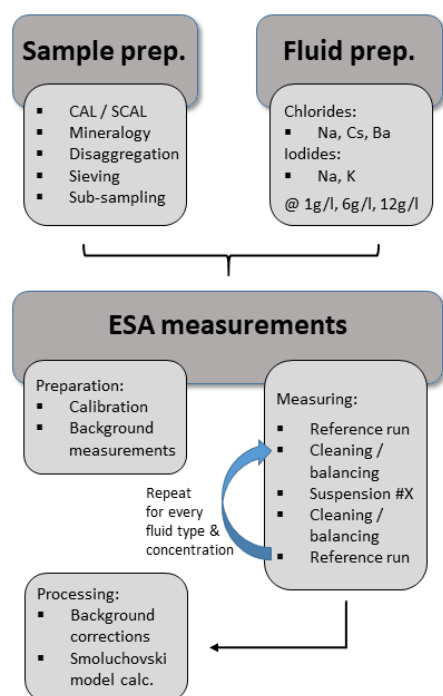


Fig. 4. Lab procedure, specifically designed for this study.

## 4 Results

### 4.1 NaCl Reference Runs

As mentioned earlier, one goal of this study was to investigate if the dopants influence the mineral surfaces in any irreversible way, especially if the dopant concentration is increased, successively. Such irreversible changes are [20]:

- **Surface charging:** Dopants can potentially alter the surface charge of mineral particles by adsorption or ion exchange, leading to changes in surface chemistry and reactivity.
- **Mineral dissolution:** Some dopants, particularly those with high solubility, could promote mineral dissolution, especially if they react with specific mineral components of the rock sample.
- **Adsorption and desorption:** Dopants adsorb onto mineral surfaces, modifying their surface properties

and potentially leading to irreversible changes if desorption is hindered.

- **Surface coating:** Dopants could form coatings on mineral surfaces, potentially affecting reactivity, and electrokinetic properties.

Figure 5 highlights the results for the reference runs, showing both uncompensated (dashed lines) and compensated (i.e., background-corrected) Smoluchowski zeta potential values (solid lines). Generally, both groups align as theoretically expected, with the uncompensated values averaging  $-7$  to  $-7.5$  mV, lower than the compensated ones averaging  $-3.5$  to  $-4$  mV. These value ranges are typical for these sandstones, with differences between each set of curves reflecting minor variations in the mineralogy of each fresh sample used [12, 21]. Nonetheless, a slight increase in zeta potential values is observed with ongoing cycles for the compensated values, a less pronounced trend but still visible for the uncompensated values. This trend aligns well with the successive loss of sample material between each cycle (about 2-3 wt%, approximately 0.075 g). Effectively, the material concentration at the end of each full dopant run (i.e., reference measurements and all concentrations of one dopant) decreased by an average of about 20 wt% (0.5 – 0.6 g). Additionally, small impurities, caused by recycling the material in between one dopant cycle have little impact.

If any dopant were to induce irreversible changes in mineral surface chemistry or properties, such alterations could potentially manifest as substantial deviations in zeta potential values, depending on the type of dopant. These deviations could lead to significantly larger or even very negative zeta potentials, reflecting the modified surface characteristics. We do not observe such evidence for our reference measurements and assume that none of the investigated dopants led to an irreversible change of surface properties. In summary, the decrease in zeta potential values observed during successive NaCl runs is likely attributed to factors as the loss of rock material, presence of small impurities, and the underlying assumptions of the background correction model (stability of the background signal, homogeneity of the suspension, and negligible interaction with the sample chamber). These factors could collectively contribute to the observed trends in zeta potential values, with the effect potentially being more pronounced in the compensated data due to the nature of the correction process.

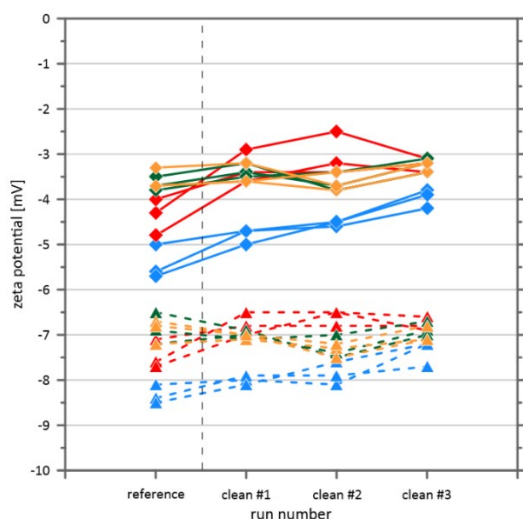


**Fig. 5.** Results of the NaCl reference measurements (i.e., of the measurements in between successively increasing dopant concentration: clean #1 = after 1g/l dopant, clean #2 = after 6g/l dopant, clean #3 = after 12 g/l dopant) for all sample types. Dashed lines indicate uncompensated, solid lines compensated Smoluchowski zeta potential values. Colour coding refers to the different dopants: blue = NaI, red = KI, green = CsCl, orange = BaCl.

#### 4.2 NaI Cycles

The sodium iodide cycles revealed a significant change in zeta potential values that is consistent for all three sandstones investigated. Figure 6 distinctly highlights these findings. Uncompensated zeta potential values range from -10 mV at the lowest to -40 mV at the highest concentration (Fig. 6, dashed lines). The compensated values (Fig. 6, solid lines) remain relatively constant, averaging around -5 mV, without showing any evidence of changes in the mineral surface or its electrokinetic behaviour.

The slightly more negative values (-6.5 mV) observed at the lowest concentration suggest a shift in the surface charge of the mineral particles. At the lowest NaI concentration (1g/l), this slight decrease in zeta potential values compared to the higher concentrations (6g/l and 12g/l) is likely attributed to the following factors [20, 21]:

- **Iodide ion concentration:** Although the overall concentration of iodide ions is lower at 1g/l compared to higher concentrations, there are still enough iodide ions present to influence the surface charge. The relatively lower concentration of iodide ions at 1g/l results in a less pronounced shift in surface charge compared to higher concentrations.
- **Surface adsorption:** At 1g/l, there is a relatively higher surface coverage of iodide ions on the mineral surface due to the lower concentration of competing ions. This increased surface coverage leads to a more

significant alteration in surface charge, resulting in the observed slightly more negative zeta potential value.

Nonetheless, the resulting (compensated) zeta potentials are more negative compared to the NaCl reference measurement at the same concentration (1g/l). This shift is likely attributed to the stronger interaction of iodide ions with the mineral surface, leading to a shift in surface charge towards more negative values due to the preferential adsorption of iodide ions over chloride ions.

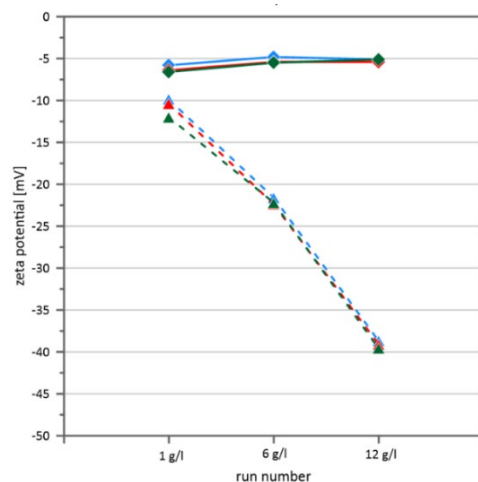


**Fig. 6.** Results of the NaI measurements for all sample types. Dashed lines indicate uncompensated, solid lines compensated Smoluchowski zeta potential values. Colour coding refers to sample type: blue = BE, red = BR, green = OK.

#### 4.3 KI Cycles

The potassium iodide cycles exhibit similar trends and observations as the sodium iodide runs. Figure 7 highlights these findings distinctly. Uncompensated zeta potential values range from -8 mV to -26.5 mV (Fig. 7, dashed lines). The compensated values (Fig. 7, solid lines) remain relatively constant, averaging around -3 mV, without showing any evidence of changes in the mineral surface or its electrokinetic behavior.

The slightly more negative values (-5 mV) observed at the lowest concentration suggest a shift in the surface charge of the mineral particles that could be attributed to similar factors as observed in the NaI runs, including the concentration of iodide ions and surface adsorption. These factors influence the composition and behavior of the electric double layer, resulting in subtle variations in the zeta potential values. Nonetheless, compensated zeta potential values are within the same range as NaCl at the lowest concentration and lower than NaI.

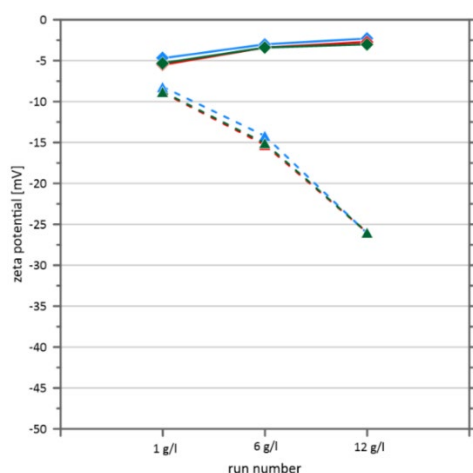


**Fig. 7.** Results of the KI measurements for all sample types. Dashed lines indicate uncompensated, solid lines compensated Smoluchowski zeta potential values. Colour coding refers to sample type: blue = BE, red = BR, green = OK.

The difference in zeta potential values between sodium iodide (NaI) and potassium iodide (KI) runs can be attributed to several factors related to the unique chemical properties of these ions and their interactions with the mineral surface [20, 21]:

- **Ion size and charge density:** Sodium ions ( $\text{Na}^+$ ) are smaller compared to potassium ions ( $\text{K}^+$ ), which results in a higher charge density for  $\text{Na}^+$  ions. As a result,  $\text{Na}^+$  ions tend to interact more strongly with the mineral surface compared to  $\text{K}^+$  ions. This stronger interaction leads to a greater alteration of the surface charge of the mineral particles, resulting in more negative zeta potential values for NaI runs compared to KI runs.
- **Adsorption behaviour:** Iodide ions ( $\text{I}^-$ ) in NaI solutions exhibit different adsorption behavior compared to iodide ions in KI solutions due to the presence of different counter ions ( $\text{Na}^+$  and  $\text{K}^+$ ). The specific adsorption of  $\text{Na}^+$  ions alongside  $\text{I}^-$  ions in NaI solutions influences the surface charge distribution on the mineral particles differently compared to KI solutions. This differential adsorption behavior can contribute to the observed differences in zeta potential values between NaI and KI runs.
- **Solution conductivity:** The conductivity of NaI solutions differs from that of KI solutions due to variations in ion mobility and concentration. Differences in solution conductivity can affect the distribution of ions near the mineral surface and, consequently, the zeta potential values. Higher solution conductivity in NaI solutions leads to stronger electrostatic interactions between ions and the mineral surface, resulting in more negative zeta potential values compared to KI solutions.
- **Solution pH:** Although both NaI and KI solutions are typically neutral, slight differences in pH exist due to the differing chemical properties of sodium and potassium ions. Variations in solution pH can influence the surface chemistry of the mineral

particles and their interaction with ions in solution, ultimately affecting zeta potential values. In our case, pH has been observed throughout the experiments and remained constant. Hence, this effect is negligible.

- **Mineral components:** The absorption behaviour of iodide ions from NaI and KI solutions towards minerals like K-feldspars, kaolinite, muscovite, and chlorite can vary based on the specific characteristics of each mineral surface and the chemical properties of the ions in solution. These differences in absorption behavior can lead to variations in surface charge and zeta potential values, highlighting the importance of considering mineral-specific interactions in interpreting these experimental results.

### 4.3 CsCl Cycles

As iodide solutions, chlorides also promote negative zeta potentials, but introduce bias for the EDL characterization and hence for interpreting possible alterations in wettability behaviour. Figure 8 illustrates this for the CsCl cycles, with uncompensated zeta potential values ranging from -10.5 mV to -70 mV. Compensated zeta potential values average around -10 mV, but indicate differences between the sample materials. This difference in compensated values between the BE sample and the combined BR and OK samples likely is attributed to variations in the interaction of Cs ions with the minerals present in each sample. Cesium ions ( $\text{Cs}^+$ ) interact differently with various mineral surfaces due to differences in their chemical properties and surface affinity. These interactions can influence the adsorption behaviour of  $\text{Cs}^+$  onto the mineral surface, consequently affecting the resulting zeta potential values. For example, certain minerals, such as illite, smectite, or muscovite, have a higher affinity for  $\text{Cs}^+$  ions due to specific surface functional groups or crystal lattice structures that facilitate stronger interactions.

Additionally, variations in the surface charge density and composition of the mineral surfaces can influence the extent of  $\text{Cs}^+$  adsorption. Minerals with higher surface charge densities or specific surface functional groups, as present within the BR and OK sample material, exhibit stronger electrostatic interactions with  $\text{Cs}^+$  ions, leading to greater adsorption and potentially affecting the resulting zeta potential values observed for each material. This observation is in very good accordance with the mineralogical composition of our sample materials (see section 2.1).

### 4.4 BaCl Cycles

The BaCl cycles exhibit similar trends and observations as the cesium chloride runs. Figure 9 highlights these



findings distinctly. Uncompensated zeta potential values range from -12 mV to -38.5 mV (Fig. 9, dashed lines). The compensated values (Fig. 9, solid lines) remain relatively constant, averaging around -7.5 mV, without showing any evidence for changes in the mineral surface or its electrokinetic behaviour.

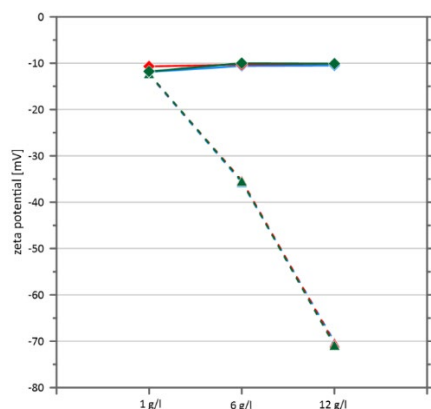


**Fig. 8.** Results of the CsCl measurements for all sample types. Dashed lines indicate uncompensated, solid lines compensated Smoluchowski zeta potential values. Colour coding refers to sample type: blue = BE, red = BR, green = OK.

The very small zeta potential change at the lowest concentration suggests a shift in the surface charge of the mineral particles that are attributed to concentration of chloride ions and surface adsorption. As for any other dopant, these factors influence the composition and behavior of the electric double layer, resulting in subtle variations in the zeta potential values. Nonetheless, we do not observe any pronounced interaction between the mineral surfaces and the dissolved  $\text{Ba}^{2+}$  ions for this cycle.

That being said, the BaCl values are less negative than those for CsCl cycles, which seems to be unexpected, considering the higher charge density of Ba ions. With two positive charges,  $\text{Ba}^{2+}$  ions possess a greater charge density than  $\text{Cs}^+$  ions, which have only one positive charge. This higher charge density results in stronger electrostatic interactions between  $\text{Ba}^{2+}$  ions and the negatively charged mineral surfaces. Therefore,  $\text{Ba}^{2+}$  ions would typically be anticipated to exhibit pronounced zeta potential values than  $\text{Cs}^+$  ions. Obviously, this is not the case here.

The difference in zeta potential values between hydrated barium chloride ( $\text{BaCl}_2$ ) and cesium chloride (CsCl) can be attributed to several factors related to the chemical properties and interactions of the respective ions with the negatively charged mineral surfaces. Firstly, despite the negatively charged mineral surface, the hydrated barium ion ( $\text{Ba}^{2+}$ ) and cesium ion ( $\text{Cs}^+$ ) possess different charge densities and hydration energies.  $\text{Ba}^{2+}$  has

a higher charge density compared to  $\text{Cs}^+$ , which causes stronger electrostatic interactions with the negatively charged mineral surfaces, resulting in relatively lower zeta potential values for  $\text{BaCl}_2$ .

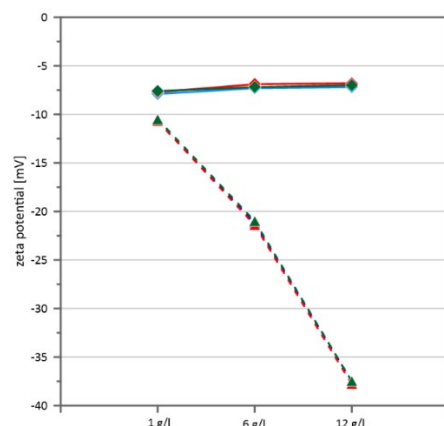


**Fig. 9.** Results of the BaCl measurements for all sample types. Dashed lines indicate uncompensated, solid lines compensated Smoluchowski zeta potential values. Colour coding refers to sample type: blue = BE, red = BR, green = OK.

Secondly, the specific adsorption behavior of  $\text{Ba}^{2+}$  and  $\text{Cs}^+$  ions onto the mineral surface differ.  $\text{Ba}^{2+}$  ions exhibit stronger adsorption onto the surface due to their higher charge density, leading to a greater reduction in the zeta potential values. On the other hand,  $\text{Cs}^+$  ions undergo weaker adsorption or compete less effectively with other ions present in the solution, resulting in relatively higher zeta potential values for CsCl. Furthermore, variations in the crystallographic structure and surface chemistry of the minerals influence the adsorption affinity of  $\text{Ba}^{2+}$  and  $\text{Cs}^+$  ions (in our case, muscovite and kaolinite, as preferentially present in BR and OK). Overall, the differences in charge density, hydration energy, and adsorption behavior between hydrated barium chloride and cesium chloride ions contribute to the observed variations in zeta potential values, with hydrated barium chloride typically exhibiting less negative values compared to cesium chloride.

## 5 Joint Discussion

After considering all the previous findings in this study, we can conclude that iodide solutions consistently yield negative zeta potential values, as chloride dopants do (see Fig. 10). That being said, neither do our results prove nor neglect the findings of [1], which demonstrated that NaI doped connate water lead to an increase in the water wettability index, indicating significantly more water-wet surfaces. Importantly, none of the dopants induces permanent, i.e., irreversible changes in surface mineralogy or EDL characteristics (refer to section 4.1

and Fig. 5). However, chlorides tend to induce surface conductivity, characterized by a non-linear relationship between zeta potentials and ionic strengths (Fig. 11 bottom half). Iodides feature a linear relationship (Fig. 11, top half), which equals a stable and consistent build-up of an EDL. The introduction of surface conductivity related effects, such as EDL screening, will bias the EDL-development and hence affect the zeta potential values. Besides, CsCl, particularly at low concentrations, exhibits on top a notable interaction with minerals possessing naturally higher surface charge density, such as mica and other clay minerals. This interaction results in increased adsorption, also potentially influencing the resulting zeta potential values (Fig. 11).

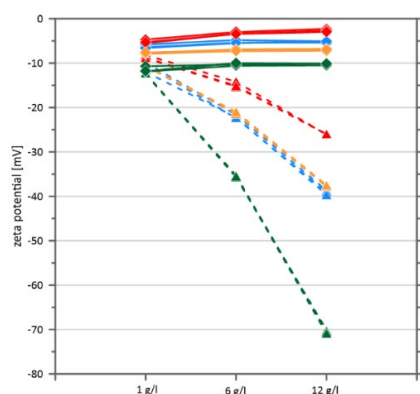


**Fig. 10.** Results for all dopants and for all sample types. Dashed lines indicate uncompensated, solid lines compensated Smoluchowski zeta potential values. Colour coding refers to dopant type: blue = NaI, red = KI, green = CsCl, orange = BaCl.

The negative zeta potential values can be linked towards more water-wet surfaces in case of this study. The electrostatic interaction between the negatively charged mineral surfaces for both, chloride and iodide ions, probably resulting in enhancing wetting behaviour, as more polar water molecules are attracted to the surface, facilitating oil displacement and improving recovery efficiency. Our results also align with the study performed by [21, 22, 23, 24]. Both, our study and the referenced papers emphasize the critical role of understanding zeta potential at mineral-water and oil-water interfaces in optimizing chemical water flooding techniques. They underscore the significance of electrostatic forces in determining the efficiency of oil recovery methods and advocate for modifying brine compositions to achieve specific zeta potential polarities, which can enhance recovery efficiency. However, they diverge in their experimental approaches and geological contexts. While our study investigates the fundamental effects of different dopants (iodides and chlorides) on zeta potential and wettability changes in sandstone, the referenced papers focus on modifying water compositions using  $\text{Ca}^{2+}$  or

$\text{Mg}^{2+}$  ions in carbonate [22, 24] and sandstone reservoirs [21, 23]. We are aware of the fact that carbonate reservoirs are chemically significantly higher reactive than conventional clastic rock reservoirs. Pairoys et al. aim for investigating carbonates in phase 2 of the ongoing research as presented in [1].

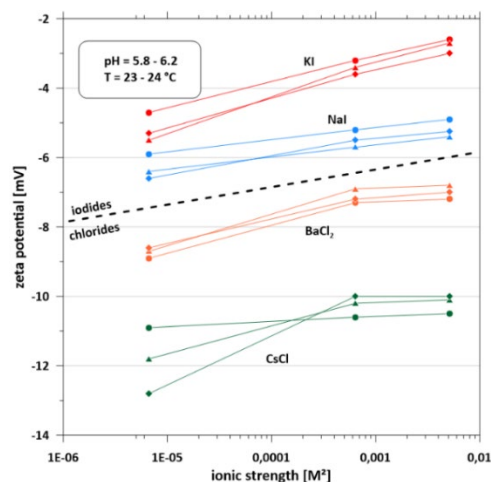


**Fig. 11.** Results for all dopants and for all sample types, and compensated Smoluchowski zeta potential values only. Concentrations are re-calculated for ionic strength. Colour coding refers to dopant type: blue = NaI, red = KI, green = CsCl, orange = BaCl.

Nevertheless, our data do not explain the greatly increased  $I_w$  for NaI doped BE-Sandstone samples, even though confirming a more water-wet behaviour. One could argue that the interfacial tension (IFT) between these fluids can play a crucial role. It refers to the force per unit length acting perpendicular to the interface between two immiscible phases, such as oil and water. In the context of oil recovery, IFT influences the behavior of oil droplets in porous rock formations, affecting their ability to flow through pore spaces and to be displaced by injected fluids. It could be assumed that the usage of especially iodide solutions decreases the IFT significantly, causing the high  $I_w$  values with increasing concentration as observed in the initial study by [1]. Nonetheless, no significant IFT reduction has been observed as first results revealed (oral communication with TotalEnergies). The overall change in IFT between the non-doped and severely doped fluid was around 1 dyn/cm and hence negligible with respect for the greatly increased  $I_w$ . This result was also reported by [28] within a systematic study related to smartwater flooding in carbonate reservoirs.

The occurrence of microbial induced films on the surface area of the SCAL samples from [1] also holds as a valid explanation. These biofilms would shield the underlying surfaces, i.e., neglecting the fluids to interact

with a mostly negatively charged grain surface. Furthermore, many biofilms inherit a positive surface charge [25], i.e., a net positive zeta potential that would favour a more oil-wet behaviour of the samples. If such a system now is doped by increasing NaI or other iodide solutions, more and more of the biofilm gets dissolved due to the significantly higher toxicity of iodide against microorganisms. This would cause a switch from net positive to net negative zeta potentials, equalling a switch from more oil-wet to significantly more water-wet. That being said the existence or non-existence of biofilms in the samples of [1] has not been investigated yet. The samples for this specific study do not feature any biofilms, but could be part of further investigations.

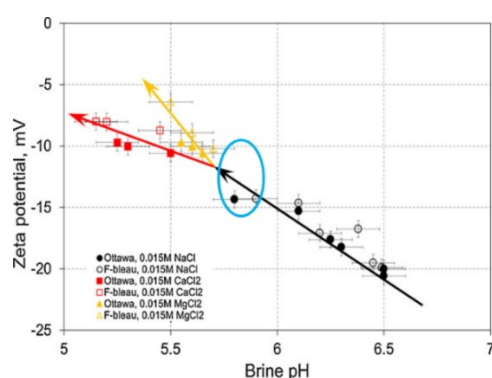


**Fig. 12.** pH dependence of zeta potentials reported by [modified after 26]. Our data align well within the observed data range (area indicated by blue ellipsoid).

Another, more reasonable explanation would be the forming of elemental iodine ( $I_2$ ) on the mineral surface reacting with the iodide ( $I^-$ ) ions, especially considering the great  $I_w$  increase when doping the connate water. Depending on the pH of the system, this elemental iodine transforms to hypoiodite ions ( $OI^-$ ) or iodate ( $IO_3^-$ ). Because these ions carry a net negative charge due to the presence of oxygen, the negatively charged mineral surface would become way more negative, i.e., the zeta potential would become way more negative, leading to a much higher increase in favourable water-wet conditions, than the presence of  $I^-$ . For getting evidence, a detailed chemical investigation of the produced brine-oil mix will support this assumption. A systematic investigation of the pH dependence of different iodide and chloride solutions concerning the EDL characterization and zeta potential change will be conducted in the near future. Nonetheless, our data align well with results published by [26] (Fig. 12).

## 6 Conclusions & Outlook

The zeta potential measurements conducted in this study serve as a crucial indicator of the electrokinetic behaviour

of mineral surfaces in various electrolyte solutions. The zeta potential is intimately linked to the electrical double layer that forms under different circumstances at the solid-liquid interface. The EDL comprises charged species attracted to the charged surface, balancing the surface charge and creating an electrostatic potential gradient known as the zeta potential. Therefore, changes in zeta potential reflect alterations in surface charge density and the composition of the EDL, which, in turn, can influence interfacial phenomena such as adsorption, dispersion, and wettability.

In case of this study, three different sandstones (BE, BR, OK) have been systematically investigated with different types of dopants (NaI, KI, CsCl, BaCl) and dopant concentrations (1 g/l, 6 g/l, 12 g/l). Linking these findings to the study initiated by [1], where the usage of NaI as dopant for enhancing imaging phase contrast coincidentally increased water-wetness, causing bias for SCAL experiments, we can conclude as follows:

### EDL-dopant interaction:

- Iodide solutions, particularly NaI and KI, promote a stable EDL and hence zeta potential development, resulting in negative zeta potentials.
- In contrast, chloride solutions, particularly CsCl and  $BaCl_2$ , show indications for induced surface conductivity at the mineral surface, especially for lower ionic strength solutions.
- Surface conductivity causes bias for the resulting zeta potentials of chloride solutions. Nonetheless, chlorides also do promote a negative zeta potential.
- CsCl potentially interferes with the rock mineralogy, especially if mica and clay minerals are present, causing bias in the EDL-characterization.
- The pH dependence of the zeta potential for these specific dopants and solutions likely plays a key role and will be investigated in phase two of this study.

### Wettability changes:

- NaI and KI treatments rendered sandstone surfaces more hydrophilic, i.e., more water-wet, due to the negative zeta potentials induced by iodide ions.
- CsCl and  $BaCl_2$  treatments, though biased by surface conductivity, formed negative zeta potentials, i.e., again promoting more water-wet conditions.
- Nonetheless, the study by [1] clearly showed the great increase in  $I_w$  for higher NaI concentrations.
- Though chlorides and iodides promote more water-wet behaviour, iodides have an greatly increased reactive potential, due to
  - its higher ionic radius,
  - higher polarizability,

- weaker bonding with water molecules,
- higher potential for redox reactions,
- which could promote stronger wettability changes, especially if pH variations are considered.
- The occurrence of microbial films, featuring a net positive surface charge (i.e., net more oil-wet surface), which shield the mineral surface underneath, could play a role for the increase in Iw values, as iodide has a higher toxicity as chloride against many bacteria. If the film disappears, surfaces will turn more water-wet.

#### General dopant feasibility for SCAL:

- Iodide solutions should be avoided, as they could drastically affect spontaneous production of oil for these types of sandstones caused by their overall higher reactive potential.
- Chloride solutions also turn these rocks more water-wet, but show a lower overall reactivity.
- Chlorides can promote surface conductivity, biasing the EDL development and hence slightly affecting wettability.
- BaCl<sub>2</sub> is favourable as long as the connate brine does not contain sulphates, causing BaSO<sub>4</sub> to precipitate.
- CsCl is favourable as long as the samples do not contain noticeable amounts of mica, illite and smectite.

For a second phase of this study, we would like to repeat this procedure for different carbonate rocks, which in most cases inherit a positively charged surface in contrast to sandstones. Furthermore, we would like to investigate the pH dependence of both rock types for these different dopant solutions used, as this parameter will affect the EDL characteristics significantly [26, 27].

The authors would like to acknowledge Dr. Stephan Kaufhold and Dr. Christian Ufer (both BGR, Hannover, Germany) for measuring and discussing the mineralogical composition of the investigated samples. Also TotalEnergies for permission to publish previous results and data shown in this work. We thank our reviewers of the SCA's Technical Board, Felix Feldmann and Kunning Tang, for reviewing and improving this manuscript.

## References

1. F. Pairoys, C. Caubit, L. Rochereau, A. Nepesov, Q. Danielczick, N. Agenet, F. Nono, *SCA Symposium Abu Dhabi - UAE*, SCA2023-007 (2023).
2. M. Arif, S.A. Abu-Khamsin, S. Iglauer, *Adv. Colloid Interface Sci.*, 268 (2019).
3. C.A. Fauziah, A.Z. Al-Yaseri, R. Beloborodov, et al. *Fuel*, 33(1) (2019).
4. M. Pooladi-Darvish, Z. Chen, K. Aziz, *Journal of Petro. Science and Engineering*, 73, 220-230 (2010).
5. K.F. Bou-Hamdan, A. H. Abbas, D.A. Martyushev, *Energies*, 16(2), p. 691ff. (2023).
6. R.J. Hunter, *Zeta Potential in Colloid Science - Principles and Applications*. Academic Press (1981).
7. G. Iler, *The Chemistry of Silica*. J. W. & Sons (1979).
8. R.R. Petrie, D.G. Shchukin, *Langmuir*, 31 (25), 6961-6971 (2015).
9. R.W. O'Brian, L.R. White, *Journal of the Chemical Society, Faraday Transactions II*, 74, p. 1607-1626 (1979).
10. P. Jungwirth, D.J. Tobias, *Chemical Reviews*, 106, 4, 1259-1281 (2006).
11. J. Newman, N.P. Balsara, *Electrochemical Systems*, 4. Wiley (2021).
12. M. Halisch, S. Kaufhold, C. Weber, *SCA Symposium 2022 Austin - Texas, USA*, SCA2022-005 (2022).
13. U. Andres, J. Jirestig, I. Timoshkin, *Powder Technology*, 104, 37-49 (1999).
14. E. Gnos, D. Kurz, I. Leya, U. Eggenberger, *Proceedings, Goldschmidt Conference* (2007).
15. R.W. O'Brian, D.W. Cannon, W.N. Rowlands, *J. of Col. and Inter. Sci.*, 173, p 406-418 (1995).
16. R. Wasche, M. Naito, V.A. Hackley, *Powder Technology*, 123(2-3), p. 275-285 (2002).
17. R.W. O'Brian, A. Jones, W.N. Rowlands, *Colloids and Surfaces A: Physicochemical and Engineering Aspects*, 218(1-3), 89-111 (2003).
18. M. Smoluchowski, *Bull. Int. Acad. Sci. Cracovie*, Vol. 184 (1903).
19. J. Lyklema, *Fundamentals of Interface and Colloid Science, Vol. II – Solid-Liquid Interfaces*. Academic Press (2011).
20. Z. Chang, X. Chen, Y. Peng, *Min. Eng.*, 121 (2018).
21. S. Li, H. Collini, M.D. Jackson, *Geophys. Res. Letters*, 45(20) (2018).
22. M.D. Jackson, D. Al-Mahrouqi, J. Vinogradov, *Nature Scientific Reports*, 6:37363 (2016).
23. M. Hidayat, M. Sarmadivaleh, J. Derksen, D. Vega-Maza, *Geophys. Res. Letters*, 49(15) (2022)
24. A. Gmira, D. Cha, A. Alghiryafi, A. Alyousef, 21<sup>st</sup> Conference Improved Oil Recovery, EAGE (2021).
25. H. Qian, Y. Cheng, C. Yang, S. Wu, *Env. Sci. and Poll. Res.*, 25(2) (2018).
26. J. Vinogradov, M.D. Jackson, M. Chamerois, *Colloids and Surfaces A*, Vol. 553 (2018)
27. E. Walker, P.W.J. Glover, *Transp. In Porous Media*, 121(1) (2018).
28. R.K. Saw, A. Mandal, *RSC Adv.*, 10, 42570-42583 (2020).